Inclusive hadron photoproduction from longitudinally polarized protons and deuterons.

P.L. Anthony, R.G. Arnold, T. Averett, H.R. Band, M.C. Berisso, H. Borel, P.E. Bosted, S.L. Bultmann, M. Buenerd, T. Chupp, et al.

Inclusive Hadron Photoproduction from Longitudinally Polarized Protons and Deuterons

The E155 Collaboration

P. L. Anthony,[16] R. G. Arnold,[1] T. Averett,[5,◇] H. R. Band,[21] M. C. Berisso,[12] H. Borel,[7] P. E. Bosted,[1] S. L. Bültmann,[19] M. Buenerd,[16,†] T. Chupp,[13] S. Churchwell,[12,‡] G. R. Court,[10] D. Crabb,[19] D. Day,[19] P. Decowski,[15] P. DePietro,[1] R. Erbacher,[16,17] R. Erickson,[16] A. Feltham,[19] H. Fonvieille,[3] E. Frlez,[19] R. Gearhart,[16] V. Ghazikhanian,[6] J. Gomez,[18] K. A. Griffioen,[20] C. Harris,[19] M. A. Houlden,[10] E. W. Hughes,[5] C. E. Hyde-Wright,[14] G. Igo,[6] S. Incerti,[3] J. Jensen,[5] J. R. Johnson,[21] P. M. King,[20] Yu. G. Kolomensky,[5,12] S. E. Kuhn,[14] R. Lindgren,[19] R. M. Lombard-Nelsen,[7] J. Marroncle,[7] J. McCarthy,[19] P. McKee,[19] W. Meyer,[4] G. S. Mitchell,[21] J. Mitchell,[18] M. Olson,[9,□] S. Penttila,[11] G. A. Peterson,[12] G. G. Petratos,[9] R. Pitthan,[16] D. Pocanic,[19] R. Prepost,[21] C. Prescott,[16] L. M. Qin,[14] B. A. Raue,[8] D. Reyna,[1,♭] L. S. Rochester,[16] S. Rock,[1] O. A. Rondon-Aramayo,[19] F. Sabatie,[7] I. Sick,[2] T. Smith,[13] L. Sorrell,[1] F. Staley,[7] S. St.Lorant,[16] L. M. Stuart,[16,§] Z. Szalata,[1] Y. Terrien,[7] A. Tobias,[19] L. Todor,[14] T. Toole,[1] S. Trentalange,[6] D. Walz,[16] R. C. Welsh,[13] F. R. Wesselmann,[14] T. R. Wright,[21] C. C. Young,[16] M. Zeier,[2] H. Zhu,[19] B. Zihlmann,[19]

[1] *American University, Washington, D.C. 20016*
[2] *Institut für Physik der Universität Basel, CH-4056 Basel, Switzerland*
[3] *University Blaise Pascal, LPC IN2P3/CNRS F-63170 Aubiere Cedex, France*
[4] *Ruhr-Universität Bochum, Universitätstr. 150, Bochum, Germany*
[5] *California Institute of Technology, Pasadena, California 91125*
[6] *University of California, Los Angeles, California 90095*
[7] *DAPNIA-Service de Physique Nucleaire, CEA-Saclay, F-91191 Gif/Yvette Cedex, France*
[8] *Florida International University, Miami, Florida 33199.*
[9] *Kent State University, Kent, Ohio 44242*
[10] *University of Liverpool, Liverpool L69 3BX, United Kingdom*
[11] *Los Alamos National Laboratory, Los Alamos, New Mexico 87545*
[12] *University of Massachusetts, Amherst, Massachusetts 01003*
[13] *University of Michigan, Ann Arbor, Michigan 48109*
[14] *Old Dominion University, Norfolk, Virginia 23529*
[15] *Smith College, Northampton, Massachusetts 01063*
[16] *Stanford Linear Accelerator Center, Stanford, California 94309*
[17] *Stanford University, Stanford, California 94305*
[18] *Thomas Jefferson National Accelerator Facility, Newport News, Virginia 23606*
[19] *University of Virginia, Charlottesville, Virginia 22901*
[20] *The College of William and Mary , Williamsburg, Virginia 23187*
[21] *University of Wisconsin, Madison, Wisconsin 53706*

We report measurements of the asymmetry $A_\parallel$ for inclusive hadron production on longitudinally polarized proton and deuteron targets by circularly polarized photons. The photons were produced via internal and external bremsstrahlung from an electron beam of 48.35 GeV. Asymmetries for both positive and negative signed hadrons, and a subset of identified pions, were measured in the momentum range $10 < P < 30$ GeV at $2.75°$ and $5.5°$. Small non-zero asymmetries are observed for the proton, while the deuteron results are consistent with zero. Recent calculations do not describe the data well.

There has been much recent interest in the spin structure of the nucleon, both theoretically and experimentally. The helicity-dependent parton distributions have been probed in a recent series of deep-inelastic polarized lepton-nucleon scattering experiments at SLAC [1], CERN [2], and DESY [3]. These experiments are primarily sensitive to the polarized quark densities, and the sensitivity to specific quark flavors can be enhanced by detecting particular mesons in coincidence with the scattered lepton (semi-inclusive measurements). It has recently been suggested [4,5] that extending such measurements to $Q^2 = 0$ (the photoproduction limit) may reveal interesting sensitivity to both the quark and gluon densities. This is because, in addition to contributions where a photon is absorbed on a quark, photons can fuse with gluons in the nucleon to produce a quark-antiquark pair, and the analyzing power for this process is large. In the ideal experiment, a monochromatic circularly polarized photon would be absorbed on a polarized proton or neutron, and an emitted pion or kaon would be detected in the final state.

In this Letter we report on measurements of inclusive hadron production by a polarized bremsstrahlung photon beam impinging on polarized proton and deuteron targets. The measurements were taken concurrently with inclusive electron scattering in SLAC E155 [1]. The polarized electron beam of energy $E_0 = 48.35$ GeV and polarization $P_e = 0.813 \pm 0.020$ passed through the polarized target, producing a bremsstrahlung photon beam with an effective flux approximately given by $\Phi(k) = (t/2)(dk/k)$, where k is the photon energy, and $t = 0.04$ and 0.02 radiation lengths (r.l.) for the NH_3 and LiD targets respectively. The electroproduction of hadrons by electrons that scatter at close to zero degrees can be considered to give an additional flux of approximately $\Phi(k) = 0.04(dk/k)$ in the effective radiator approximation. Since only the helicity-dependent asymmetry for hadron photoproduction is measured in this experiment, it is not important to know the magnitude of the photon flux. The photon circular polarization is given by [6] $P_\gamma/P_e = y(4 - y)/(4 - 4y + 3y^2)$, where $y = k/E_0$. This formula yields values of P_γ/P_e of 1, 0.91, 0.64, and 0.29 for $y = 1$, 0.75, 0.5, and 0.25, respectively, illustrating that the photons are the most polarized near the endpoint.

The longitudinally polarized proton target was a 3-cm-long cell filled with granules of $^{15}NH_3$ immersed in liquid He at 1 K in a uniform magnetic field of 5 T. The proton polarization varied from 0.6 to 0.9 during the experiment, with a typical value of $P_t = 0.8$. A small ($< 2\%$) correction was made to the asymmetry measurements for the polarization of the ^{15}N nuclei. Crystals of ^{6}LiD were used for the deuteron target, in which the ^{6}Li nuclei were treated as an effective polarized deuteron with 86% of the polarization of the free deuteron [7], which averaged about $P_t = 0.22$ during the experiment. The polarization

directions of both the NH_3 and LiD targets were periodically reversed to cancel out possible false asymmetries.

Charged particles leaving the target at laboratory angles of approximately 2.75 or 5.5 degrees were detected in two independent magnetic spectrometers, each with a momentum acceptance of 10 to 40 GeV. The detector systems were similar in the two spectrometers, consisting of two highly segmented planes of plastic scintillator hodoscopes for tracking, and an array of 200 lead glass blocks used for additional tracking information as well as energy measurements. Electron showers were fully contained in these 24 r.l. blocks, while hadrons typically deposited one third of their energy in the several interaction lengths of the lead glass. The ratio of lead glass energy E to particle momentum P was found to be a useful quantity in distinguishing electrons from hadrons, as illustrated in Fig. 1. Almost all electrons are characterized by $E/P > 0.8$, while about 80% of the hadrons are characterized by $E/P < 0.6$. The peak near $E/P = 0.07$ is from muons and non-showering hadrons, both depositing about 0.7 GeV in the lead glass array. Also useful for particle identification were the two several-meter-long gas threshold Cherenkov counters in each spectrometer. The nitrogen gas pressure in each tank was set for thresholds of 69 (58) MeV for electrons, corresponding to 14 (12) GeV for muons, 19 (16) GeV for pions, 57 (48) GeV for kaons, and 133 (112) GeV for protons in the 2.75 (5.5) degree spectrometer. These thresholds were chosen to correspond to the point where the pion to electron ratio drops below unity (see Fig. 2). The efficiency of the Cherenkov counters was approximately 95% for electrons, while the probability of a hadron below Cherenkov threshold to produce one or more photoelectrons was reduced to less than 1% by the addition of 10% methane to quench scintillation light.

The readout of all the detectors was done once per beam pulse (120 Hz), with hodoscope and lead glass hits registered in multi-hit TDCs, the lead glass energies recorded in ADCs, and the time distribution of each Cherenkov counter response digitized in flash-ADCs at 1 nsec time intervals. Unlike other SLAC experiments which used specific triggers to selectively record electron events, the present system allowed most of the much more copious hadron tracks and shower clusters to be reconstructed in addition to the electron candidates.

Fig. 2 shows the calculated ratio of positrons, muons, pions, kaons, and (anti-)protons rates to electron rates, for both the negative and positive polarity spectrometer settings (approximately 20% of the data were taken with the positive settings). The hadron rates are from a fit to previous lower energy data [8]. These predictions are in good agreement with the PYTHIA Monte Carlo [9], except for the K^+ rate, which is lower in PYTHIA by a factor of two. The rates are only for pions and kaons that do not decay in the 40 (25) m active length of the 2.75 (5.5) degree spectrometer. The electron rates are from

a standard fit to deep-inelastic electron scattering data [10], and include radiative tail effects. The positron rates are from the PYTHIA Monte Carlo for decay sources (the most important being π^0 and J/ψ decay), and a Bethe-Heitler code [11] for the pair production contribution. The muons come primarily from decay of pions and kaons in flight, with additional contributions from Bethe-Heitler and J/ψ decay at high transverse momenta.

Although the detector systems were very good at identifying electrons in the presence of a large hadron flux, the identification of different hadrons is not particularly good. We therefore developed one set of cuts to define inclusive hadrons, and a more restricted set of cuts to identify a sample that is almost entirely pions. The set of cuts we used to identify inclusive hadrons was $E > 1.5$ GeV (to eliminate muons), $E/P < 0.6$ (to remove electrons and positrons), $P < 29$ (24) GeV at $2.75°$ ($5.5°$), and that the lead glass cluster not be near the edge of the array (to avoid leakage out the sides). For this "hadron" definition, the Cherenkov information was ignored. The upper momentum cut was found to be necessary because the hadron cross section drops very rapidly with increasing momentum, and contributions from a variety of background processes begin to dominate above the momentum cut used. Using the rates shown in Fig. 2, the remaining "hadron" sample then consists of roughly 95% pions for the negative sample, and about 70% for the positive sample, with the remainder about equally divided among protons and kaons. The "pion" definition required both Cherenkov counters to have a signal, and the momentum to be above 19 (16) GeV (pion Cherenkov threshold), in addition to the cuts used for the "hadron" definition.

Within the uncertainties of the detector efficiencies, the ratio of total hadron to electron rates was observed to be consistent with the predictions shown in Fig. 2. The ratio of positive to negative hadrons in the momentum range 10 to 20 GeV was observed to be approximately constant at 1.3 in both spectrometers and for both targets, in rough agreement with the predictions of Fig. 2.

The helicity-dependent asymmetries were determined according to:

$$A_\parallel = \left(\frac{N_- - N_+}{N_- + N_+}\right)\frac{1}{f'P_bP_t}, \qquad (1)$$

where positive target polarization is defined to be parallel to the electron beam direction, N_- (N_+) is number of detected hadrons per incident charge for negative (positive) beam helicity, and f' is the dilution factor representing the fraction of measured events originating from polarizable protons or deuterons within the target (including the effective deuteron in ^{6}Li). The asymmetry $A_\parallel$ has previously been designated E [12] in the literature. In calculating f', we assumed the yield of hadrons per nucleon to be independent of atomic number A. Possible shadowing

corrections were looked for by parameterizing the cross section per nucleon as A^α. Using data taken periodically during the experiment with targets of carbon, beryllium, empty cup (mostly aluminum), and empty cup filled with helium, we found $\alpha = 0.0 \pm 0.1$ for both spectrometers in the momentum range $10 < P < 20$, where the hadron rates are highest. We used values of $f' = 0.13 \pm 0.03$ for the NH_3 target and $f' = 0.34 \pm 0.04$ for the LiD target. The large error bars on f' are dominated by the large uncertainty in the nuclear dependence of the hadron yields, compared to the much better known A-dependence for deep inelastic electron scattering.

The results for $A_\parallel$ are displayed in Fig. 3 for the proton target, and Fig. 4 for the deuteron target, for both positive and negative signed hadrons in each spectrometer. Both the inclusive hadron and identified pion definitions are shown. The errors shown are statistical only. The relative systematic errors are approximately 20% (12%) for the proton (deuteron) target, dominated by the uncertainty in f'. The results for the proton show a significant positive asymmetry, which is twice as large for positive hadrons as for negative hadrons in a given spectrometer. The transverse momentum range in the 2.75 degree spectrometer is $0.5 < P_t < 1.5$ GeV, half that of the 5.5 degree spectrometer. No significant difference is seen between the inclusive hadron and identified pion results, although the later covers a more restrictive momentum range, and has larger statistical errors.

The inclusive hadron asymmetries for the proton target are much smaller than the corresponding asymmetries for deep inelastic electrons (about 0.08 (0.16) for the 2.75 (5.5) degree spectrometer). Several checks were made (for example, by changing the E/P cuts) to ensure that the small, non-zero asymmetries are not due to contamination of electrons or muons mis-identified as hadrons. As a check against possible false asymmetries, it was verified that the physics asymmetry remains constant when the sign of the target polarization was reversed, either by changing the direction of the magnetic field, or by changing the microwave frequency used in dynamic nuclear polarization. The results for the deuteron target are all consistent with zero. Taken together, the deuteron and proton results imply a small negative asymmetry for polarized neutrons. Negative asymmetries were in fact observed for a polarized neutron target in both spectrometers in experiment E154 [13], with an average value of $A_\parallel = -0.004 \pm 0.001$ for negative hadrons, and $A_\parallel = -0.008 \pm 0.002$ for positive hadrons, averaged over the full momentum range of both spectrometers. The results for both proton and deuteron targets are also consistent with the results for SLAC E143 [14], taken at lower beam energies but with considerably larger statistical errors.

Also shown in Figs. 3 and 4 are some of the calculations [4] made to match the experimental conditions of the 5.5 degree spectrometer. The loose dotted, tight dot-

ted, and dashed curves all use the BBS polarized gluon distribution [15], with three commonly used polarized quark distribution functions. The solid curve is the same as the loose dotted curve, but has $\Delta G(x) = 0$. The calculations were not done for the 2.75 degree spectrometer due to the low average P_t, where Vector Meson Dominance contributions might be expected to become important. The calculations take into account the energy and polarization dependence of the photon spectrum, but are only for pions. This should not make much difference for the negative signed hadrons, which are almost all pions, as indicated in Fig. 2. The calculations are done in leading order perturbative QCD and take into account direct contributions, pions from fragmentation of quarks and gluons, and resolved photon contributions. For the range $10 < P < 20$ GeV where we have good measurements of $A_\parallel$, the fragmentation process is dominant. Since this includes quarks produced via the photon-gluon fusion subprocess, for which the analyzing power is very large, there is expected to be good sensitivity to the polarized gluon distribution, compared to measurements of g_1, where the gluon polarization does not contribute in leading order. To compare with our deuteron data, we have naively taken the average of the predicted asymmetries for neutron and proton targets.

In general, the calculations predict larger asymmetries than observed experimentally, especially for the positive hadrons from the proton target. In this case, the differences between the curves are less than the differences between any of the curves and the data. This makes it impossible to draw any conclusions about $\Delta G(x)$. The calculations for the deuteron do predict smaller asymmetries than for the proton, as observed experimentally, but also tend to be higher than the data for positive hadrons. None of the choices of quark and gluon polarization are in good agreement with our entire data set. It is possible that soft processes, not easily calculable in perturbative QCD, are playing a more significant role than expected in the calculations. Extending the calculations to NLO and the inclusion of soft processes (in progress by the authors of [4]) may also lead to better agreement with the data. Ideally, the calculations should also include kaons and protons in the final state. It thus remains as an interesting theoretical challenge to calculate the full gamut of processes in inclusive polarized hadron photoproduction. The present data will provide valuable experimental constraints on such models, and perhaps lead to constraints on the gluon polarization in the nucleon in the future.

◇   Present address: College of William and Mary, Williamsburg, VA 23187

†   Permanent Address: Institut des Sciences Nucléaires, IN2P3/CNRS, 38026 Grenoble Cedex, France

‡   Present Address: Duke University, TUNL, Durham, NC 27708

▫   Present Address: Saint Norbert College, DePeke, WI 54115

♭   Present Address: DESY, D-22603, Hamburg, Germany

§   Present Address: Lawrence Livermore National Laboratory, Livermore, CA 94551

[1] SLAC E155, P. L. Anthony *et al.,* SLAC–PUB–7983 (hep–ex/9901006); SLAC-PUB-7994; SLAC–PUB–8041.

[2] SMC, D. Adeva *et al.,* Phys. Rev. D58 (1998) 112001.

[3] HERMES, A. Airapetian *et al.,* Phys. Lett. B442 (1998) 484.

[4] A. Afanasev, C. E. Carlson, C. Wahlquist, Phys. Rev. D 58 (1998) 054007.

[5] D. De Florian and W. Vogelsang, Phys. Rev. D 57 (1998) 4376; B. A. Kniehl, hep-ph/9709261; M. Stratmann and W. Vogelsang, hep-ph/9708243.

[6] H. Olsen and L. C. Maximon, Phys. Rev. 110 (1958) 589.

[7] S. L. Bültmann *et al.,* SLAC-PUB-7904 (1998); O. A. Rondon, Report No. aps1998dec15_002 (1998), submitted to Phys. Rev. C.

[8] D. Wiser, PhD thesis, University of Wisconsin, 1977 (unpublished). Fit available from S. Rock (ser@slac.stanford.edu).

[9] T. Sjostrand, Computer Physics Comm. 82 (1994) 74.

[10] NMC, P. Arneodo *et al.,* Phys. Lett. B364 (1995) 107.

[11] Y. S. Tsai, Rev. Mod. Phys. 46 (1974) 815; 49 (1977) 421 (E); R. Yoshida, Nucl. Instrum. Meth. A302 (1991) 63.

[12] I. S. Barker, A. Donnachie, and S. K. Storrow, Nucl. Phys. B95 (1975) 347.

[13] F. Sabatie, PhD Thesis, DAPNIA/SPhN-9803T (1998); Yu. G. Kolomensky, PhD thesis, University of Massachusetts (1997), (unpublished).

[14] SLAC E143, K. Abe *et al.,* Phys. Rev. D58 (1998) 112003.

[15] S. J. Brodsky, M. Burkardt, and I. Schmidt, Nucl. Phys. B441 (1995), 197.
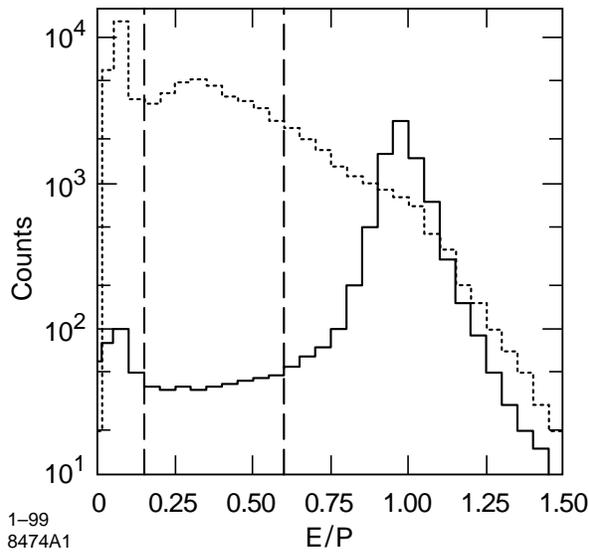
FIG. 1. Number of counts as a function of the ratio of calorimeter energy E to track momentum P for a typical 1 hour data run with the 5.5 degree spectrometer set in negative polarity. The solid curve is for the case where both Cherenkov counters had significant pulse height (mostly electrons), while the dashed curve is for the case where the Cherenkov counters had zero or small pulse height (mostly pions, kaons, and muons). The momentum range is restricted to $10 < P < 15$ GeV. The vertical dashed lines approximately show the cuts used to define the hadron sample.
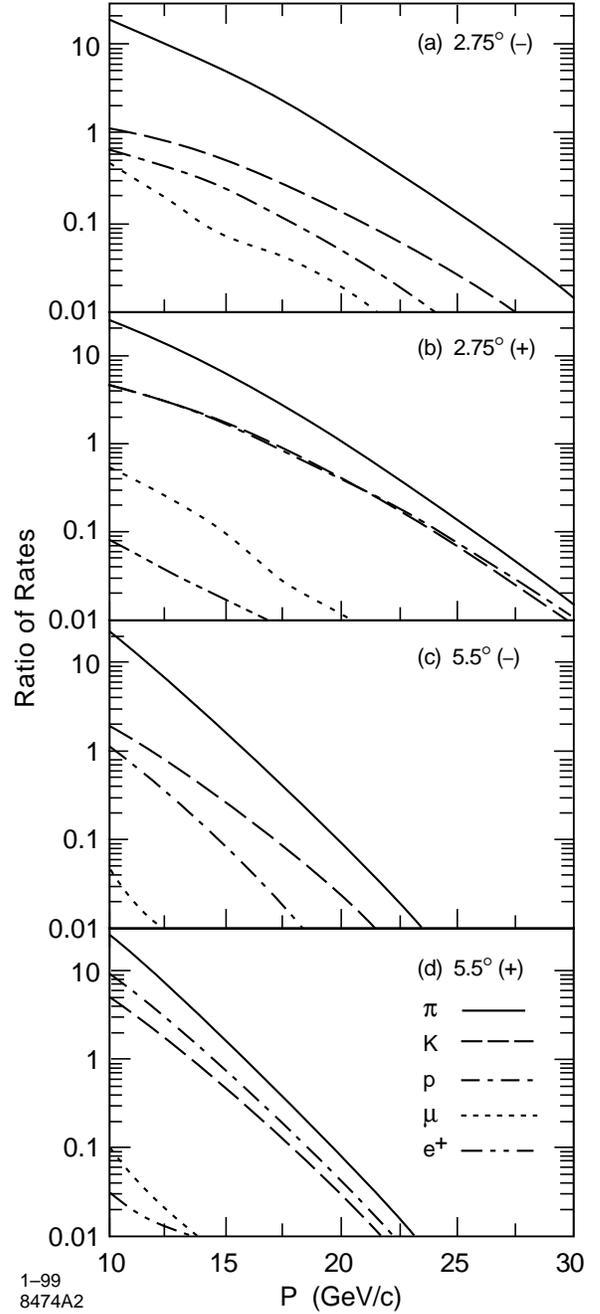
FIG. 2. Predicted ratio of rates of particles to the corresponding electron rate in each spectrometer, for positive and negative particles. The hadron rates are from Ref. [8].

5
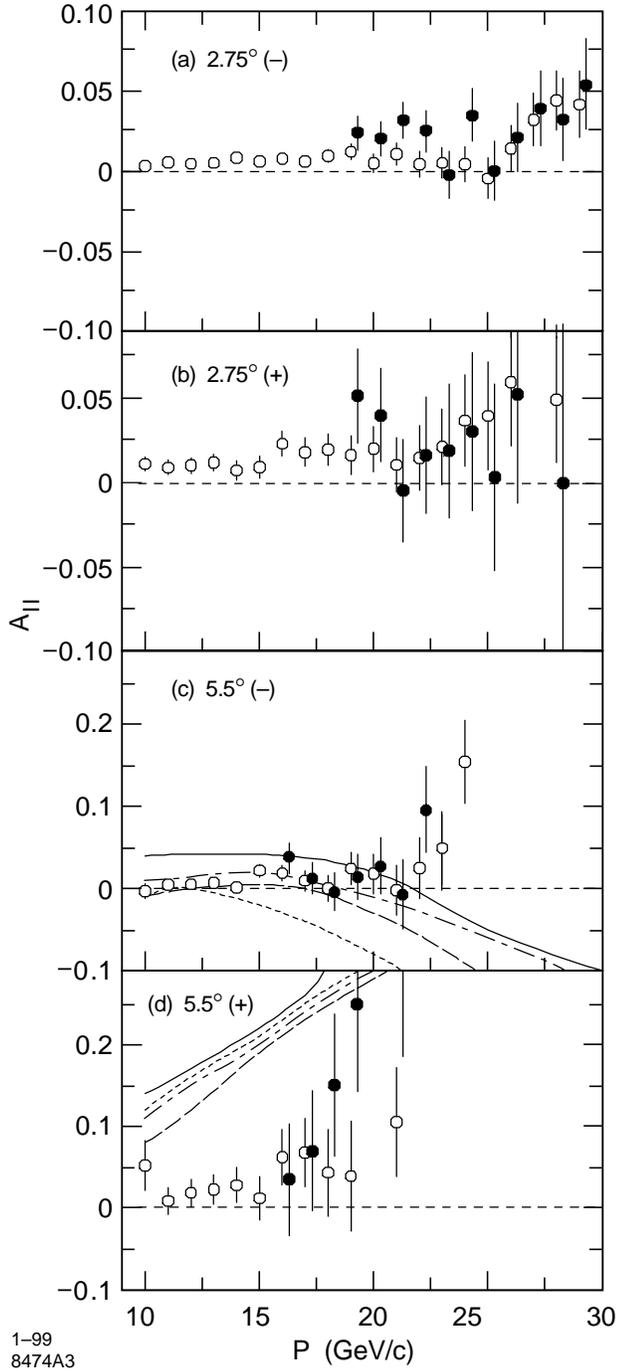
FIG. 3. The helicity-dependent asymmetries $A_\parallel$ for polarized photoproduction of inclusive hadrons (open circles) and pions (solid circles) from a longitudinally polarized proton, for both spectrometers and for both positive (+) and negative (-) particles. The 5.5 degree curves are taken from Fig. 9 of Ref. [4].
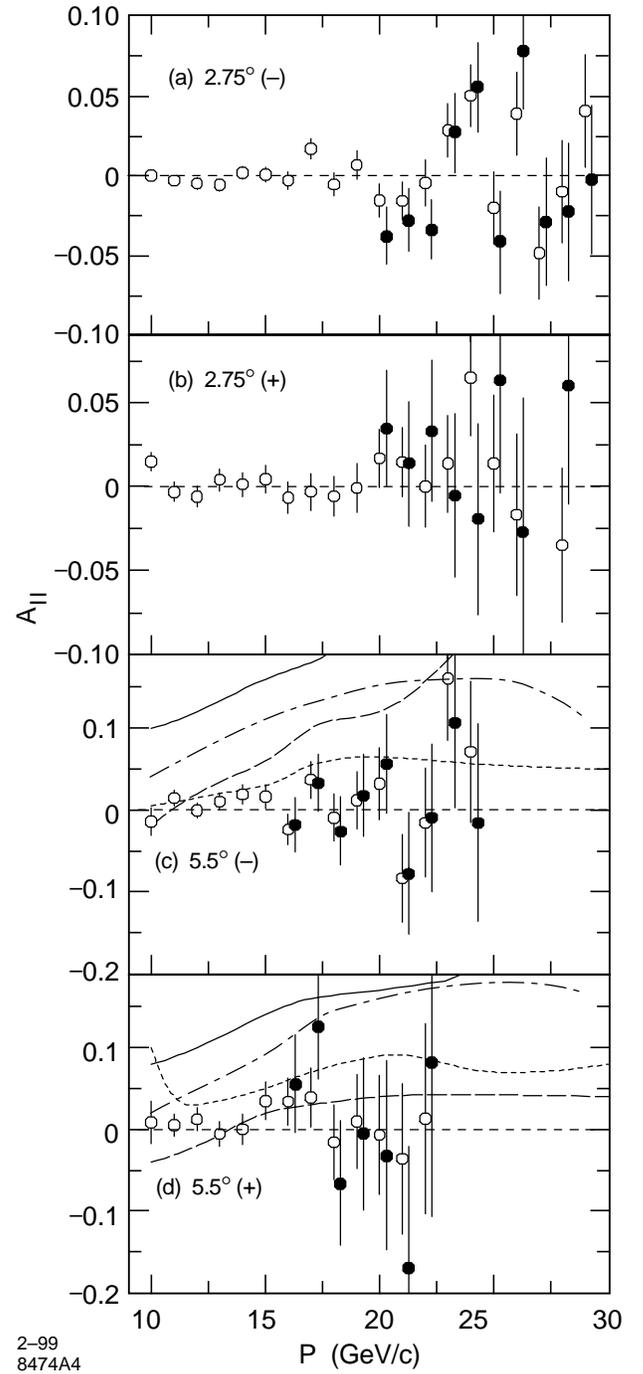
FIG. 4. Same as Fig. 3 except for a polarized deuteron target. The 5.5 degree curves are an average of the neutron (Fig. 8) and proton (Fig. 9) calculations of Ref. [4].

TABLE I. The helicity-dependent asymmetries $A_{\parallel}$ for polarized photoproduction of inclusive hadrons from a longitudinally polarized proton, for both spectrometers and for both positive (h^+) and negative (h^-) particles. The photon endpoint energy is 48.35 GeV. The errors are statistical only.

$P(GeV)$	$\theta = 2.75^\circ\ h^-$	$\theta = 2.75^\circ\ h^+$	$\theta = 5.5^\circ\ h^-$	$\theta = 5.5^\circ\ h^+$
10.0	0.003 ± 0.002	0.011 ± 0.004	-0.003 ± 0.009	0.052 ± 0.031
11.0	0.006 ± 0.002	0.009 ± 0.004	0.005 ± 0.005	0.009 ± 0.016
12.0	0.005 ± 0.002	0.010 ± 0.005	0.005 ± 0.005	0.019 ± 0.017
13.0	0.005 ± 0.002	0.012 ± 0.005	0.007 ± 0.006	0.023 ± 0.018
14.0	0.009 ± 0.002	0.007 ± 0.006	0.001 ± 0.006	0.028 ± 0.022
15.0	0.006 ± 0.003	0.009 ± 0.006	0.022 ± 0.008	0.012 ± 0.027
16.0	0.008 ± 0.003	0.023 ± 0.007	0.019 ± 0.010	0.062 ± 0.033
17.0	0.006 ± 0.004	0.018 ± 0.008	0.010 ± 0.012	0.068 ± 0.042
18.0	0.010 ± 0.004	0.020 ± 0.009	0.000 ± 0.016	0.044 ± 0.053
19.0	0.012 ± 0.005	0.017 ± 0.012	0.024 ± 0.020	0.039 ± 0.067
20.0	0.005 ± 0.006	0.020 ± 0.014	0.018 ± 0.024	-
21.0	0.011 ± 0.007	0.011 ± 0.016	-0.002 ± 0.030	0.105 ± 0.067
22.0	0.005 ± 0.008	0.015 ± 0.019	0.025 ± 0.038	-
23.0	0.005 ± 0.009	0.021 ± 0.023	0.050 ± 0.044	-
24.0	0.005 ± 0.011	0.037 ± 0.027	0.155 ± 0.051	-
25.0	-0.004 ± 0.013	0.040 ± 0.032	-	-
26.0	0.014 ± 0.015	0.060 ± 0.038	-	-
27.0	0.033 ± 0.017	-	-	-
28.0	0.045 ± 0.018	0.049 ± 0.037	-	-
29.0	0.042 ± 0.021	-	-	-

TABLE II. Same as Table I, but for identified pions.

$P(GeV)$	$\theta = 2.75^\circ\ \pi^-$	$\theta = 2.75^\circ\ \pi^+$	$\theta = 5.5^\circ\ \pi^-$	$\theta = 5.5^\circ\ \pi^+$
16.0	-	-	0.037 ± 0.018	0.035 ± 0.068
17.0	-	-	0.013 ± 0.020	0.070 ± 0.073
18.0	-	-	-0.004 ± 0.023	0.151 ± 0.087
19.0	0.024 ± 0.011	0.052 ± 0.028	0.014 ± 0.028	0.249 ± 0.107
20.0	0.021 ± 0.011	0.040 ± 0.028	0.028 ± 0.034	-
21.0	0.032 ± 0.011	-0.005 ± 0.031	-0.007 ± 0.042	0.304 ± 0.119
22.0	0.025 ± 0.013	0.016 ± 0.034	0.096 ± 0.053	-
23.0	-0.002 ± 0.015	0.019 ± 0.040	-	-
24.0	0.035 ± 0.016	0.031 ± 0.047	-	-
25.0	0.001 ± 0.019	0.003 ± 0.055	-	-
26.0	0.021 ± 0.021	0.053 ± 0.065	-	-
27.0	0.040 ± 0.024	-	-	-
28.0	0.033 ± 0.026	0.096 ± 0.065	-	-
29.0	0.055 ± 0.028	-	-	-

TABLE III. Same as Table I, but for deuteron target.

$P(GeV)$	$\theta = 2.75^\circ$ h^-	$\theta = 2.75^\circ$ h^+	$\theta = 5.5^\circ$ h^-	$\theta = 5.5^\circ$ h^+
10.0	0.000 ± 0.003	0.015 ± 0.006	-0.014 ± 0.017	0.009 ± 0.026
11.0	-0.003 ± 0.003	-0.003 ± 0.006	0.015 ± 0.009	0.005 ± 0.014
12.0	-0.005 ± 0.003	-0.006 ± 0.006	-0.001 ± 0.009	0.012 ± 0.014
13.0	-0.006 ± 0.004	0.004 ± 0.007	0.010 ± 0.010	-0.005 ± 0.016
14.0	0.002 ± 0.004	0.001 ± 0.007	0.019 ± 0.012	0.000 ± 0.018
15.0	0.001 ± 0.005	0.004 ± 0.008	0.016 ± 0.015	0.035 ± 0.023
16.0	-0.003 ± 0.005	-0.007 ± 0.009	-0.024 ± 0.018	0.034 ± 0.029
17.0	0.017 ± 0.006	-0.003 ± 0.011	0.037 ± 0.023	0.039 ± 0.036
18.0	-0.006 ± 0.007	-0.006 ± 0.012	-0.009 ± 0.029	-0.016 ± 0.046
19.0	0.007 ± 0.009	-0.001 ± 0.015	0.012 ± 0.035	0.009 ± 0.058
20.0	-0.016 ± 0.010	0.017 ± 0.017	0.032 ± 0.044	-0.007 ± 0.072
21.0	-0.016 ± 0.012	0.015 ± 0.020	-0.083 ± 0.054	-0.036 ± 0.092
22.0	-0.005 ± 0.014	0.000 ± 0.024	-0.015 ± 0.066	0.013 ± 0.116
23.0	0.028 ± 0.017	0.014 ± 0.029	0.161 ± 0.076	-
24.0	0.050 ± 0.019	0.065 ± 0.034	0.071 ± 0.086	-
25.0	-0.020 ± 0.022	0.014 ± 0.041	-	-
26.0	0.039 ± 0.026	-0.017 ± 0.048	-	-
27.0	-0.049 ± 0.029	-	-	-
28.0	-0.010 ± 0.032	-0.035 ± 0.046	-	-
29.0	0.041 ± 0.035	-	-	-

TABLE IV. Same as Table III, but for identified pions.

$P(GeV)$	$\theta = 2.75^\circ$ π^-	$\theta = 2.75^\circ$ π^+	$\theta = 5.5^\circ$ π^-	$\theta = 5.5^\circ$ π^+
16.0	-	-	-0.018 ± 0.033	0.056 ± 0.060
17.0	-	-	0.033 ± 0.035	0.126 ± 0.064
18.0	-	-	-0.026 ± 0.042	-0.065 ± 0.076
19.0	-	-	0.018 ± 0.050	-0.005 ± 0.093
20.0	-0.038 ± 0.018	0.035 ± 0.034	0.056 ± 0.061	-0.032 ± 0.116
21.0	-0.028 ± 0.020	0.014 ± 0.037	-0.077 ± 0.074	-0.169 ± 0.149
22.0	-0.034 ± 0.022	0.033 ± 0.042	-0.010 ± 0.090	0.082 ± 0.188
23.0	0.026 ± 0.025	-0.005 ± 0.049	0.107 ± 0.104	-
24.0	0.055 ± 0.028	-0.020 ± 0.057	-0.016 ± 0.121	-
25.0	-0.042 ± 0.032	0.063 ± 0.067	-	-
26.0	0.078 ± 0.036	-0.027 ± 0.080	-	-
27.0	-0.029 ± 0.040	-	-	-
28.0	-0.023 ± 0.043	0.060 ± 0.071	-	-
29.0	-0.003 ± 0.047	-	-	-